

Supplementary Information for

Hydrothermally Self-templated Synthesis of Rectangular Polyimide Submicrotubes and Promising Potentials in Electrochemical Energy Storage

*Sheng Lei,[‡] Xun Cui,[‡] Xufei Liu, Xiaofang Zhang, Xiaoyan Han, and Yingkui Yang**

Key Laboratory of Catalysis and Energy Materials Chemistry of Ministry of Education & Hubei Key Laboratory of Catalysis and Materials Science, South-Central University for Nationalities, Wuhan 430074, China

E-mail: ykyang@mail.scuec.edu.cn

[‡] Both S. Lei and Dr. X. Cui contribute equally to this work.

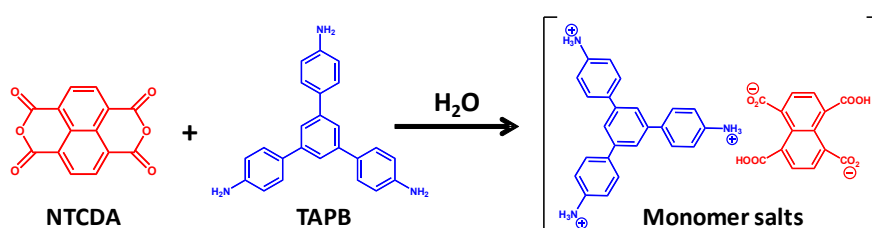
Experimental section

Materials

1,4,5,8-naphthalene-tetracarboxylic acid dianhydride (NTCDA) was purchased from Sigma Aldrich. 1,3,5-Tris(4-aminophenyl)benzene (TAPB) was bought from Shanghai Yuanye Bio-technology Co Ltd., China. *N*-methyl-2-pyrrolidone (NMP) and mesitylene were supplied by Sinopharm Chemical Reagent Beijing Co Ltd., China. Isoquinoline was purchased from Aladdin Co Ltd., China. All chemicals were directly used without further purification.

Synthesis of monomer salts

NTCDA (0.402 g, 1.5 mmol) was dispersed in 15.0 mL deionized water and stirred at 80°C for 1 h in an Ar atmosphere. TAPB (0.351 g, 1.0 mmol) was then added under stirring for another 2 h. The yellow powder was obtained by filtration and washing with deionized water and ethanol, and finally dried at 60°C in vacuum for 12 h.



Scheme S1. Synthetic route of monomer salts.

Synthesis of polyimides

The monomer salt was dispersed in 30.0 mL deionized water and then transferred into a Teflon-lined autoclave. The autoclave was placed in an oven at 200°C for 12 h. After cooling down to room temperature, the resultant reaction mixture was filtered followed by washing with deionized water and ethanol for several times. The product was finally obtained by drying overnight at 80°C. In control experiments, the polycondensation of monomer salts was also performed in a Teflon-lined autoclave filled with different volume ratio of NMP to water under identical experimental conditions.

Synthesis of *N*-doped carbon tubes

N-Doped carbon tubes (NCTs) were easily prepared by thermal pyrolysis of the as-synthesized polyimide tubes at 800°C for 2 h under an argon flowing.

Materials characterization

Scanning electron microscopy (SEM) images were acquired from the SU 8010 microscope, and transmission electron microscopy (TEM) tests were examined on a Tecnai G20 electron microscope. Fourier transform infrared (FT-IR) spectra were determined on a Thermo Nicolet Nexus 470 spectrometer. Thermogravimetric analysis (TGA) was performed on a TG209 F3 instrument under N₂ at 10°C min⁻¹.

Powder X-ray diffraction (XRD) patterns were recorded on a PANalytical Empyrean diffractometer in the range of $2\theta = 5\text{-}80^\circ$ using a monochromatic $\text{Cu K}\alpha$ radiation.

Electrochemical measurements

For LIBs, electrochemical performance was examined at room temperature using CR2032 coin-type half cells. The electrode was fabricated by mixing PITs, carbon black (Super P), and polyvinylidene fluoride (5:4:1 in weight ratio) in NMP to form a slurry. The resultant slurry was coated on an Al foil (for cathode) and a Cu foil (for anode), respectively. NMP was carefully removed by vacuum-drying at 80°C overnight. The electrode film was punched into disks with a diameter of 10 mm. The mass loading of PITs on each piece of electrode is around 1.0 mg cm^{-2} . The half-cells were then assembled by using the lithium foil as the counter electrode, porous membrane Celgard 2400 as the separator, and 1 M lithium bis(trifluoromethanesulfonyl) imide in 1,3-dioxolane and 1,2-dimethoxyethane (1:1 in volume) as the electrolyte. Galvanostatic charge-discharge (GCD) measurements were performed on a LAND CT2001A automatic battery system in the voltage range of 1.5–3.5 V (vs Li^+/Li) for the cathode and 0.01–3.0 V (vs Li^+/Li) for the anode, respectively. Cyclic voltammetry (CV) and electrochemical impedance spectroscopy (EIS) tests were carried out on a CHI 760E electrochemical workstation (Chenhua Instrument Co., Shanghai) in the same voltage range.

For supercapacitors, the symmetric coin-type devices were assembled by using two identical NCT electrodes and measured on a CHI 660E electrochemical workstation. The working electrodes were fabricated by mixing NCTs, super P, and polytetrafluoroethylene (8:1:1 in weight ratio) in isopropanol. An aqueous solution of 1 M H_2SO_4 and filter paper were utilized as the electrolyte and separator, respectively. Both CV, and GCD curves were recorded in the potential range of -0.2 to 0.8 V under the scan rates of 10 to 300 mV s^{-1} and the applied current densities of 1 to 20 A g^{-1} .

Supplementary figures

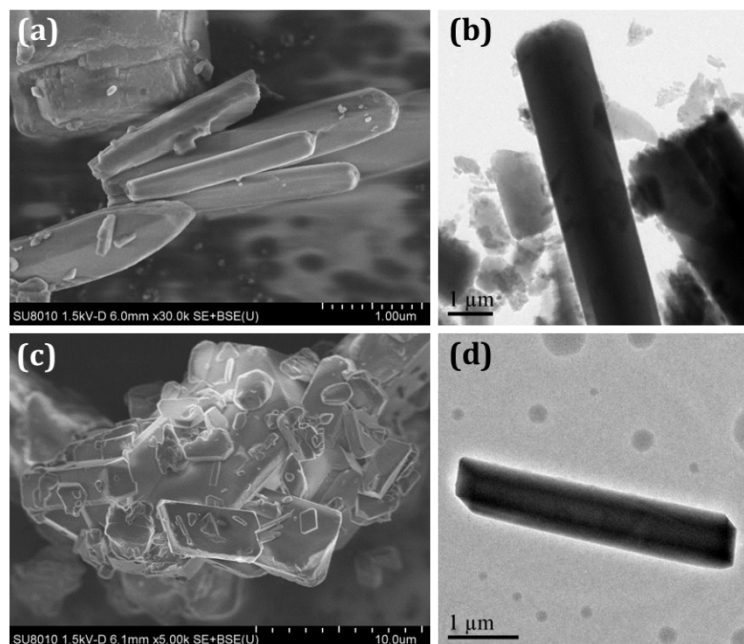


Fig. S1 SEM (a, c) and TEM (b, d) images of (a, b) NTCDA and (c, d) TAPB monomers.

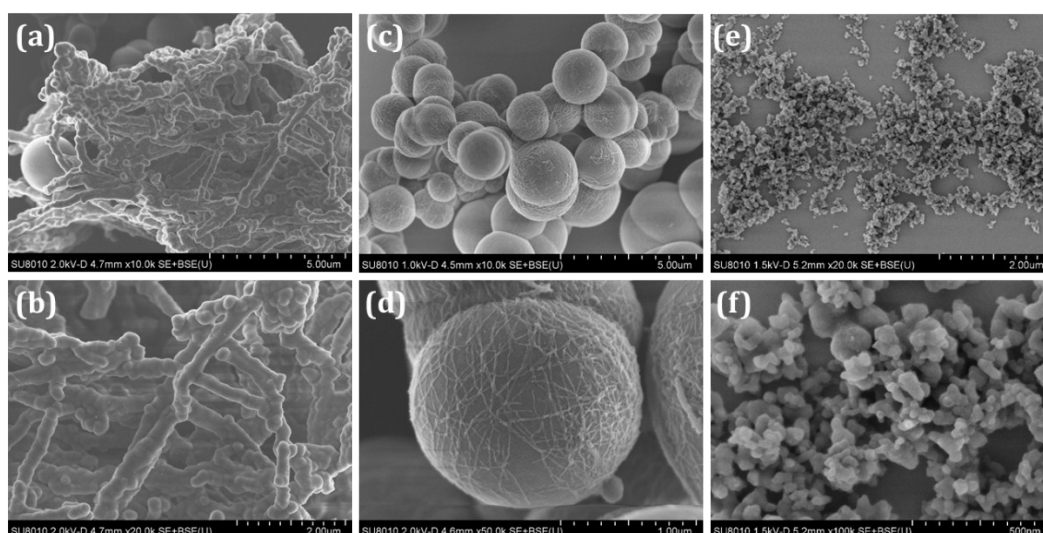


Fig. S2 SEM images of polyimides produced by polycondensation reactions of monomer salts in different volume ratio of NMP to water ($V_{\text{NMP}/\text{W}}$) of (a, b) $V_{\text{NMP}/\text{W}}=1:2$, (c, d) $V_{\text{NMP}/\text{W}}=1:1$, and (e, f) $V_{\text{NMP}/\text{W}}=1:0$.

The control experiments were carried out to reveal the possible mechanism of PITs. Considering that the reaction media play an important role in assembling the morphologies of polymers during the synthesis process,^[1,2] the polycondensation of NTCDA-TAPB monomer salts was performed in a Teflon-lined autoclave filled with different volume ratio of *N*-methyl pyrrolidone (NMP) to water ($V_{\text{NMP/W}}$). The addition of NMP to water ($V_{\text{NMP/W}}=1:2$) led to the formation of a protuberance-threaded rod morphology (**Fig. S2a, b†**), while micron-sized spheres covered with nanowires of ca. 15 nm (**Fig. S2c, d†**) were clearly observed at the $V_{\text{NMP/W}}$ of 1:1. However, nanoparticles with about 50 nm in diameter (**Fig. S2e, f†**) were produced when NMP was used ($V_{\text{NMP/W}}=1:0$), corresponding to the solvothermally-synthesized polyimide. Furthermore, monomer salts are well soluble in NMP and hardly soluble in water (**Fig. S3†**). The solubility parameter (δ) of polyimide is ca. $30.0 \text{ (MPa)}^{1/2}$ (**Table S1†**), which is between $22.9 \text{ (MPa)}^{1/2}$ for NMP and $47.8 \text{ (MPa)}^{1/2}$ for water.^[3] The δ difference between polyimide and water is thus greater, suggesting the weaker interaction between the two.^[2] The as-synthesized polyimide is also insoluble in water. These results reasonably reveal that water plays a critical role in forming PITs.

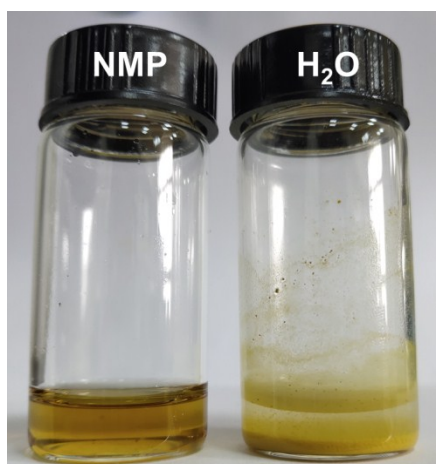


Fig. S3 Optical picture of monomer salts dissolved in NMP and water.

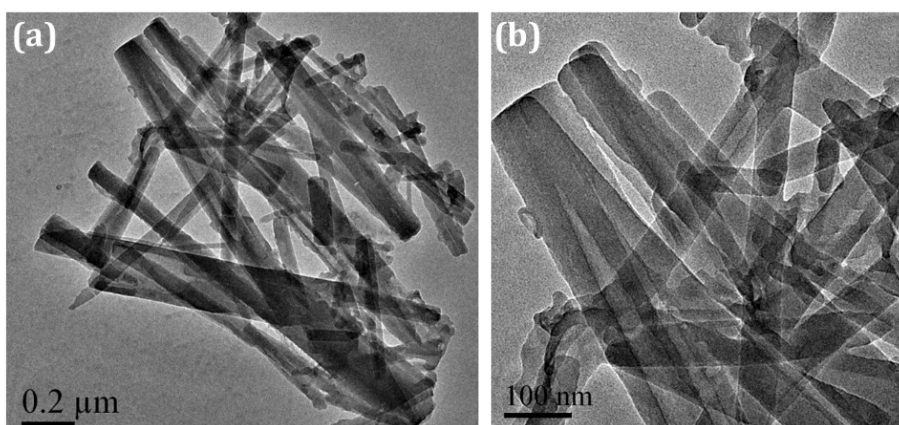


Fig. S4 TEM images of hydrothermally-synthesized products at 200°C for 1 h.

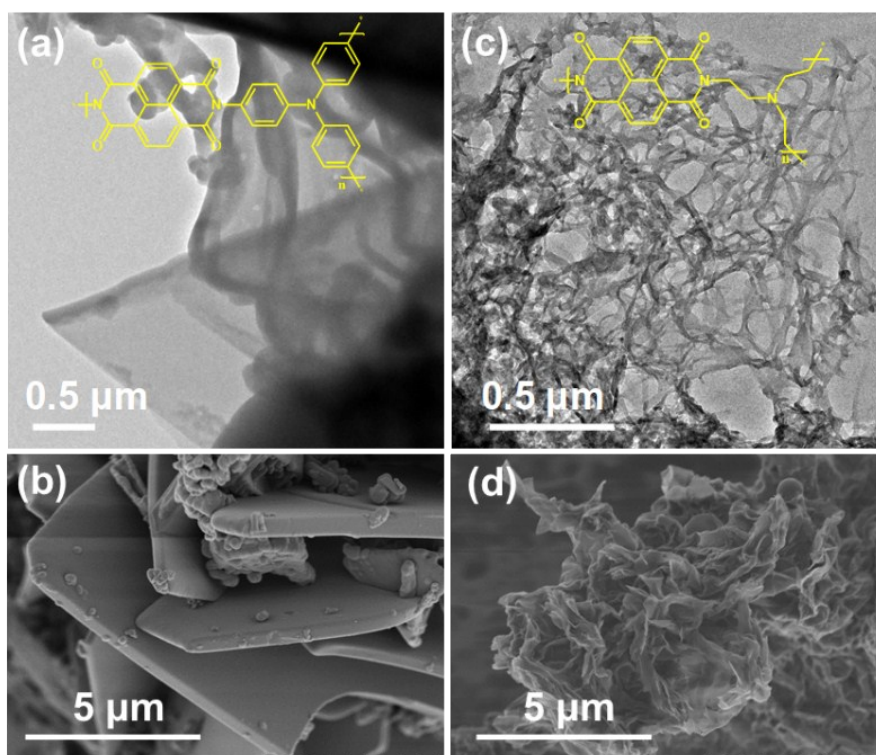


Fig. S5 TEM (a, c) and SEM (b, d) images of polyimides produced by hydrothermal polycondensation of monomer salts of NTCDA with (a, b) tris(4-aminophenyl) amine and (c, d) tris(2-aminoethyl) amine instead of TAPB.

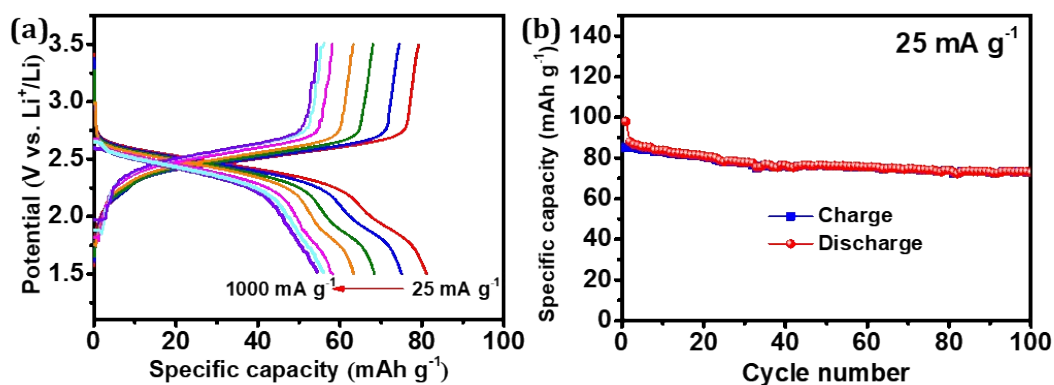


Fig. S6 (a) Charge/discharge profiles of the PIT cathode under different current densities, and (b) cycling stability of the PIT cathode evaluated at a current density of 25 mA g^{-1} .

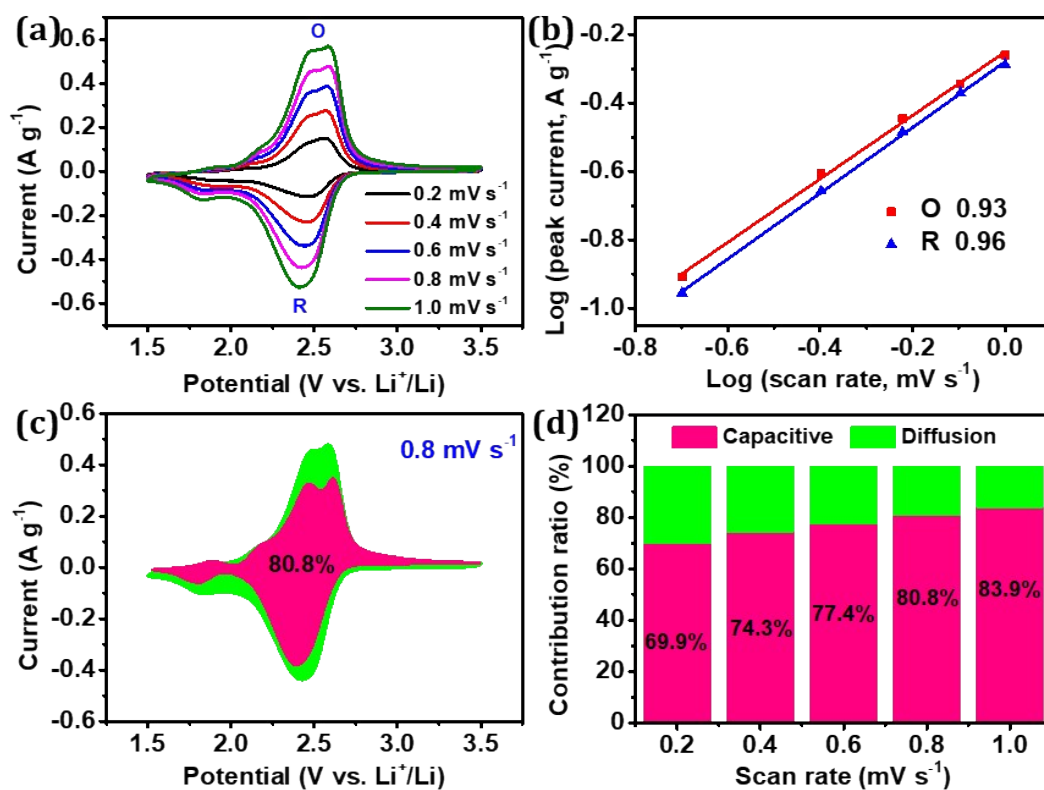


Fig. S7 Electrochemical kinetics and reaction mechanism analysis: (a) CV curves of the PIT cathode under different scan rates, (b) the $\log(i)$ versus $\log(v)$ plots and the fitting b -value of redox peaks, (c) typical capacitive contribution of the PIT cathode at 0.8 mV s^{-1} , and (d) the normalized capacitive and diffusion-controlled contribution ratios at different scan rates.

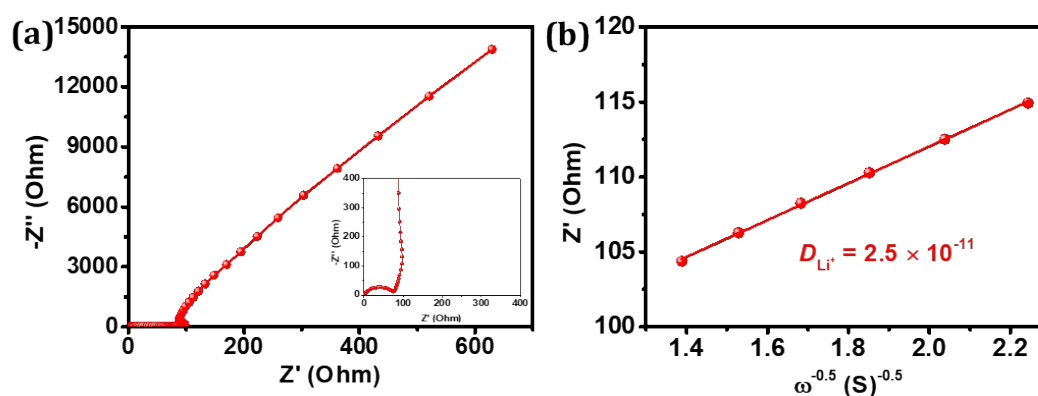


Fig. S8 (a) Nyquist plots of the PIT cathode, and (b) the plots of real parts of complex impedance vs $\omega^{-1/2}$.

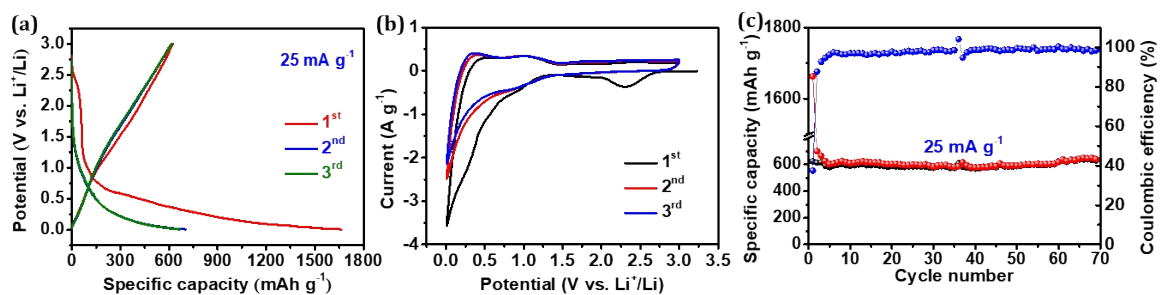


Fig. S9 Electrochemical performance of the PIT anode: (a) charge-discharge curves at 25 mA g^{-1} , and (b) CV profiles at 1.0 mV s^{-1} in the first three cycles, and (c) cycling stability at 25 mA g^{-1} .

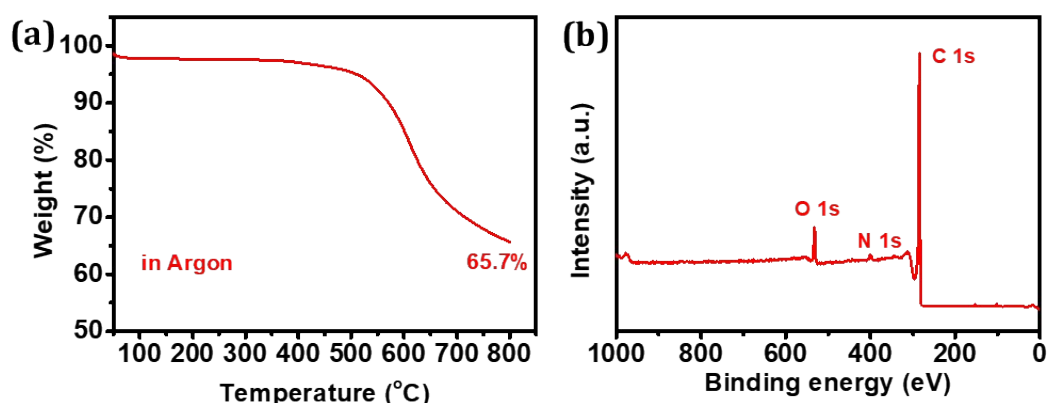


Fig. S10 (a) TGA curve of PITs tested in an Ar atmosphere, and (b) typical XPS spectra of NCTs derived from thermal pyrolysis of PITs.

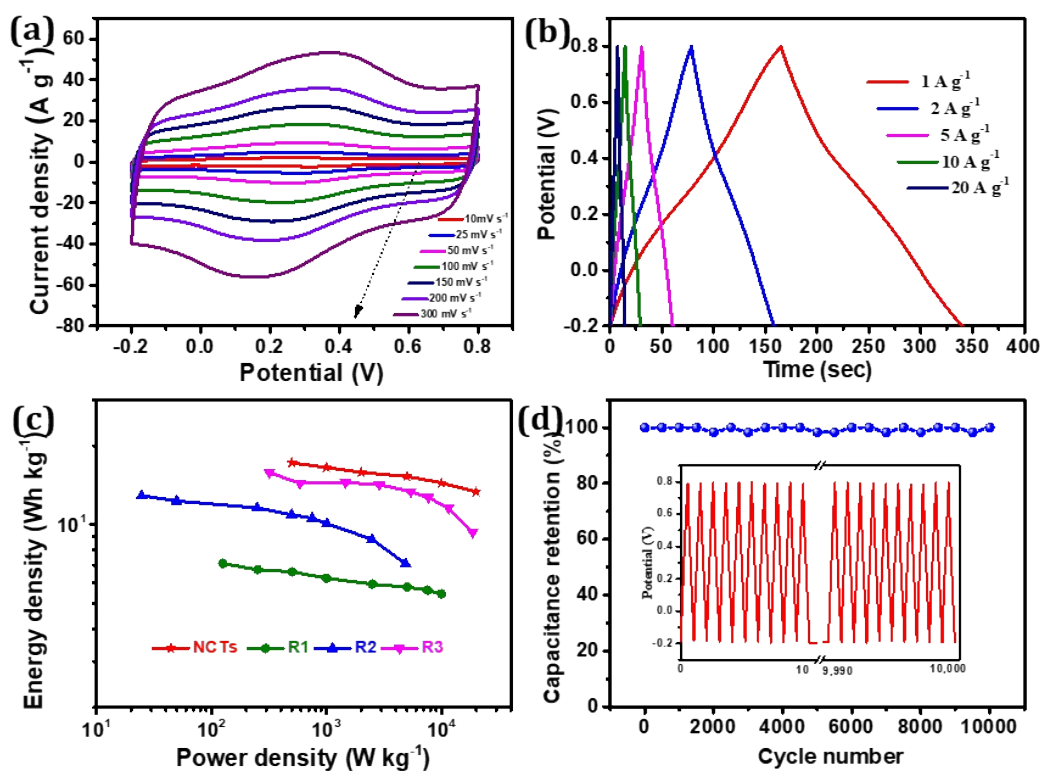
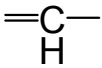
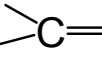
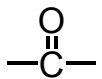
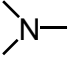


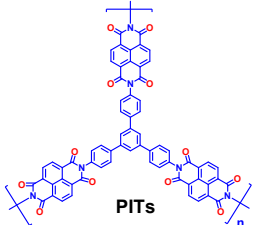
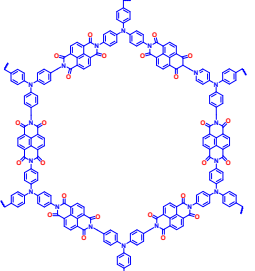
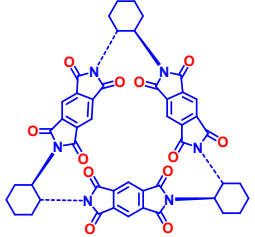
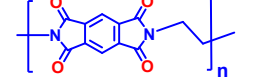
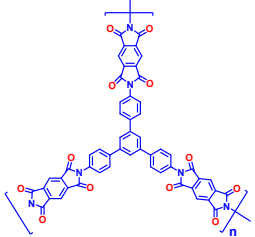
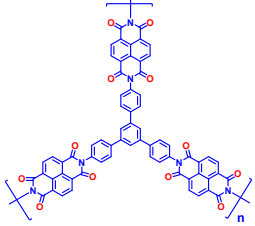
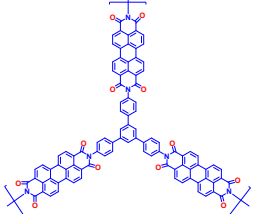
Fig. S11 (a) CV curves under different scan rates and GCD curves under current densities of the NCT electrode in a three-electrode system. Electrochemical performance of symmetric supercapacitors-based NCTs: (c) Ragone plots and the previously reported supercapacitors, and (d) cycling stability running at 20.0 A g⁻¹ for 10 000 cycles (the insets show GCD curves for the initial and last ten cycles). References: R1^[4], R2^[5], and R3^[6].


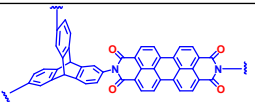
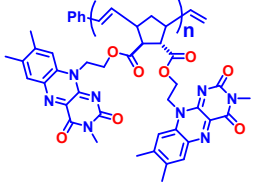
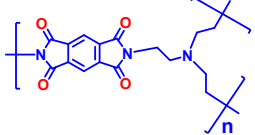
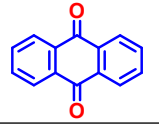
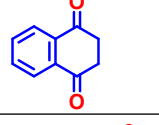
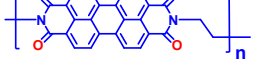
Table S1. Solubility parameter of PITs calculated by the group contribution method.^[7,8]

Group parameter	<i>n</i>	$\Delta E_{\text{Coh},i}$ (J mol ⁻¹)	ΔV_i (cm ³ mol ⁻¹)
	2	4310	13.5
	2	4310	-5.5
	4	17370	10.8
	2	4190	-9
Phenylene (o, m, p)	3	31940	52.4
Phenyl (trisubstituted)	1	31940	33.4
Phenyl (tetrasubstituted)	1	31940	14.4
Ring closure 5 or more atoms	3	1050	16
Conjugation in ring for each double bond	2	1670	-2.2
SUM		261290	289.8

$$\delta = \left(\frac{\Delta E_{\text{Coh},i}}{\Delta V_i} \right)^{\frac{1}{2}} = (261290/289.8)^{1/2} = \mathbf{30.0} \text{ [J cm}^{-3}\text{]}^{1/2}$$

Table S2. A survey of electrochemical performance of the PIT cathode for LIBs and other polymer cathodes reported previously

Materials	Specific capacity	Rate capability	Capacity retention	C=O utilization	Ref.
 PITs	80.5 mAh g ⁻¹ at 25 mA g ⁻¹	56.5 mAh g ⁻¹ at 1.0 A g ⁻¹	90.2% after 100 cycles at 25 mA g ⁻¹ 70.3% after 15000 cycles at 1.5 A g ⁻¹	70%	This work
	28.5 mAh g ⁻¹ at 100 mA g ⁻¹	-	100% after 50 cycles at 100 mA g ⁻¹	22.6%	[9]
	126 mAh g ⁻¹ at 0.2 C	65 mAh g ⁻¹ at 2 C	75.0% after 30 cycles at 0.2 C	-	[10]
	175 mAh g ⁻¹ at 44.3 mA g ⁻¹	36 mAh g ⁻¹ at 2.2 A g ⁻¹	82.0% after 150 cycles at 221.5 mA g ⁻¹	39.5%	[11]
	36 mAh g ⁻¹ at 25 mA g ⁻¹	-	-	21.3%	[12]*
	97 mAh g ⁻¹ at 25 mA g ⁻¹	-	66.2% after 30 cycles at 25 mA g ⁻¹	66.4%	
	78 mAh g ⁻¹ at 25 mA g ⁻¹	-	74.1% after 65 cycles at 25 mA g ⁻¹	71.4%	

	85 mAh g ⁻¹ at 50 mA g ⁻¹	0 mAh g ⁻¹ at 200 mA g ⁻¹	88.2% after 50 cycles at 50 mA g ⁻¹	65.8%	[13]
	75.9 mAh g ⁻¹ at 4.8 mA g ⁻¹	22.4 mAh g ⁻¹ at 482 mA g ⁻¹	80.2% after 500 cycles at 193 mA g ⁻¹	78.7%	[14]
	53 mAh g ⁻¹ at 150 mA g ⁻¹	25 mAh g ⁻¹ at 3.0 A g ⁻¹	28.0% after 200 cycles at 144 mA g ⁻¹	-	[15]
	160 mAh g ⁻¹ at 38.3 mA g ⁻¹	74 mAh g ⁻¹ at 3.83 A g ⁻¹	86.6% after 200 cycles at 191.5 mA g ⁻¹	-	[16]
	-	-	-	45.6%	[17]
	-	-	100% after 100 cycles at 0.05C	40.5%	
	134.9 mAh g ⁻¹ at 25 mA g ⁻¹	50 mAh g ⁻¹ at 9.9 A g ⁻¹	87.5% after 5000 cycles at 198 mA g ⁻¹	54.3%	[18]

* Polyimides nanoparticles were synthesized by refluxing of NTCDA and TAPB in N, N-dimethylformamide (DMF) at 170~180°C for 20~24 hours under the catalysis of propionic acid.^[12]

References

1. X. F. Liu, P. Mei, S. Lei, X. F. Zhang, Q. Liu and Y. K. Yang, *Energy Technol.*, 2019, 1901013.
2. Z. Xu, X. Zhuang, C. Yang, J. Cao, Z. Yao, Y. Tang, J. Jiang, D. Wu and X. Feng, *Adv. Mater.*, 2016, **28**, 1981
3. A. F. M. Barton, *Chem. Rev.*, 1975, **75**, 731.
4. L. F. Chen, X. D. Zhang, H. W. Liang, M. Kong, Q. F. Guan, P. Chen, Z. Y. Wu and S. H. Yu, *ACS Nano*, 2012, **6**, 7092.
5. T. E. Rufford, D. H. Jurcakova, Z. H. Zhu and G. Q. Lu, *Electrochem. Commun.*, 2008, **10**, 1594.
6. Q. Wang, J. Yan, Y. B. Wang, T. Wei, M. L. Zhang, X. Y. Jing and Z. J. Fan, *Carbon*, 2014, **67**, 119.
7. D. Karst and Y. Q. Yang, *J. Appl. Polym. Sci.*, 2005, **96**, 416.
8. K. Y. Chun, S.H. Jang, H.S. Kim, Y.W. Kim, H.S. Han and Y. Joe, *J. Membrane. Sci.*, 2000, **169**, 197.
9. G. Wang, N. Chandrasekhar, B. P. Biswal, D. Becker, S. Paasch, E. Brunner, M. Addicoat, M. Yu, R. Berger and X. L. Feng, *Adv. Mater.*, 2019, 1901478.
10. D. J. Kim, K. R. Hermann, A. Prokofjevs, M. T. Otlej, C. Pezzato, M. Owczarek and J. F. Stoddart, *J. Am. Chem. Soc.*, 2017, **139**, 6635.
11. Y. Meng, H. Wu, Y. Zhang and Z. Wei, *J. Mater. Chem. A*, 2014, **2**, 10842.
12. D. Tian, H. Z. Zhang, D. S. Zhang, Z. Chang, J. Han, X. P. Gao and X. H. Bu, *RSC Adv.*, 2014, **4**, 7506.
13. P. Sharma, D. Damien, K. Nagarajan, M. M. Shaijumon and M. Hariharan, *J. Phys. Chem. Lett.*, 2013, **4**, 3192.
14. T. B. Schon, A. J. Tilley, E. L. Kynaston and D. S. Seferos, *ACS Appl. Mater. Inter.*, 2017, **9**, 15631.
15. T. B. Schon, A. J. Tilley, C. R. Bridges, M. B. Miltenburg and D. S. Seferos, *Adv. Funct. Mater.*, 2016, **26**, 6896.
16. H. Wu, Q. Meng, Q. Yang, M. Zhang, K. Lu and Z. Wei, *Adv. Mater.*, 2015, **27**, 6504.
17. Y. Ding, Y. Li and G. Yu, *Chem.*, 2016, **1**, 790.
18. H. G. Wang, S. Yuan, D. L. Ma, X. L. Huang, F. L. Meng and X. B. Zhang, *Adv. Energy Mater.*, 2014, **4**, 1301651.